Tracheobronchial transplantation with a stem-cell-seeded bioartificial nanocomposite: a proof-of-concept study

Philipp Jungebluth, Evren Alici, Silvia Baiguera, Katarina Le Blanc, Pontus Blomberg, Béla Bozóky, Claire Crowley, Oskar Einarsson, Karl-Henrik Grinnemo, Tomas Gudbjartsson, Sylvie Le Guyader, Gert Henriksson, Ola Hermanson, Jan Erik Juto, Bertil Leidner, Tobias Lilja, Jan Liska, Tom Luedde, Vanessa Lundin, Guido Moll, Bo Nilsson, Christoph Roderburg, Staffan Strömblad, Tolga Sutlu, Ana Isabel Teixeira, Emma Watz, Alexander Seifalian, Paolo Macchiarini

Summary

Background **Tracheal tumours can be surgically resected but most are an inoperable size at the time of diagnosis; therefore, new therapeutic options are needed. We report the clinical transplantation of the tracheobronchial airway with a stem-cell-seeded bioartificial nanocomposite.**

Methods **A 36-year-old male patient, previously treated with debulking surgery and radiation therapy, presented with recurrent primary cancer of the distal trachea and main bronchi. After complete tumour resection, the airway was replaced with a tailored bioartificial nanocomposite previously seeded with autologous bone-marrow mononuclear cells via a bioreactor for 36 h. Postoperative granulocyte colony-stimulating factor filgrastim (10 µg/kg) and epoetin beta (40 000 UI) were given over 14 days. We undertook flow cytometry, scanning electron microscopy, confocal microscopy epigenetics, multiplex, miRNA, and gene expression analyses.**

Findings **We noted an extracellular matrix-like coating and proliferating cells including a CD105+ subpopulation in the scaffold after the reseeding and bioreactor process. There were no major complications, and the patient was asymptomatic and tumour free 5 months after transplantation. The bioartificial nanocomposite has patent anastomoses, lined with a vascularised neomucosa, and was partly covered by nearly healthy epithelium. Post-operatively, we detected a mobilisation of peripheral cells displaying increased mesenchymal stromal cell phenotype, and upregulation of epoetin receptors, antiapoptotic genes, and miR-34 and miR-449 biomarkers. These findings, together with increased levels of regenerative-associated plasma factors, strongly suggest stem-cell homing and cell-mediated wound repair, extracellular matrix remodelling, and neovascularisation of the graft.**

Interpretation **Tailor-made bioartificial scaffolds can be used to replace complex airway defects. The bioreactor reseeding process and pharmacological-induced site-specific and graft-specific regeneration and tissue protection are key factors for successful clinical outcome.**

Funding **European Commission, Knut and Alice Wallenberg Foundation, Swedish Research Council, StratRegen, Vinnova Foundation, Radiumhemmet, Clinigene EU Network of Excellence, Swedish Cancer Society, Centre for Biosciences (The Live Cell imaging Unit), and UCL Business.**

Introduction

Primary tracheal cancers are rare neoplastic lesions characterised by a high mortality rate. The gold standard treatment for these lesions is surgical resection with primary reconstruction.[1] However, epidemiological studies have shown that, because of difficulties in the definitive diagnosis, most patients with primary malignant tracheal cancers present with local inoperable disease (exceeding 6 cm or >50% of the total tracheal length) and are, therefore, treated with palliative measures. For these patients, prognosis is poor with a reported 5-year survival rate of about 5%.[2] Moreover, because safe reconstruction of the trachea is not possible, even in patients with operable tumours, the proportion of complete tumour resection is less than 60%.[3] This outcome would be greatly improved if a trachea substitute with similar anatomical, physiological, and biomechanical properties of the native trachea were available.

In 2008, we reported the first fully tissue-engineered tracheal transplantation with a non-immunogenic decellularised human donor trachea reseeded with bone-marrow-derived mesenchymal stem cells (MSCs) and respiratory cells.[4] However, this approach is limited by the shortage of donor organs of an appropriate size and has other disadvantages (webappendix p 9). As a result, an alternative, tailor-made synthetic tracheal scaffold is an urgent clinical need. We report the clinical transplantation of the tracheobronchial airway in a patient with recurrent primary trachea cancer, with use of a tailor-made artificial scaffold reseeded ex vivo with mononuclear cells (MNCs)[5] and a growth factor-induced endogenous stem cells mobilisation.

Methods

The recipient

Webappendix pp 2–9 provides a detailed description of the methods. A 36-year-old man presented in May, 2011,

Lancet 2011; 378: 1997–2004

Published Online November 24, 2011 DOI:10.1016/S0140-6736(11)61715-7

See Comment page 1977

Advanced Center for Translational Regenerative Medicine (P Jungebluth MD, S Baiguera PhD, K-H Grinnemo MD, Prof P Macchiarini MD), **Cell and Gene Therapy Centre, Department of Medicine, Division of Hematology** (E Alici MD, T Sutlu BSc), **Departments of Medicine and Laboratory Medicine** (Prof K Le Blanc MD, G Moll MS, E Watz MD), **Center for Biosciences, Department of Biosciences and Nutrition** (S Le Guyader PhD, Prof S Strömblad PhD), **Linnaeus Center in Developmental Biology for Regenerative Medicine, Department of Neuroscience** (O Hermanson PhD, T Lilja PhD), **Department for Clinical Science, Intervention and Technology** (B Leidner MD), **Department of Cell and Molecular Biology** (V Lundin MS, A I Teixeira PhD), **and European Airway Institute** (Prof P Macchiarini), **Karolinska Institutet, Stockholm, Sweden; Division of Ear, Nose and Throat** (P Jungebluth, Prof P Macchiarini, G Henriksson MD, J E Juto MD), **Vecura, Clinical Research Center** (P Blomberg PhD), **Division of Pathology** (B Bozóky MD), **Department of Cardiothoracic Surgery and Anesthesiology** (K-H Grinnemo, J Liska MD), **Department of Radiology (Huddinge)** (B Leidner MD), **and Department of Clinical Immunology and Transfusion Medicine** (E Watz), **Karolinska University Hospital, Stockholm, Sweden; Centre for Nanotechnology and Regenerative Medicine,**

University College London, London, UK (C Crowley MSc, Prof A Seifalian PhD); **Department of Pulmonology** (O Einarsson MD) **and Department of Cardiothoracic Surgery** (Prof T Gudbjartsson MD), **Landspitali University Hospital, Faculty of Medicine, University of Iceland, Reykjavik, Iceland; Department of Medicine 3, University Hospital RWTH Aachen, Aachen, Germany** (T Luedde MD, C Roderburg MD); **and Rudbeck Laboratory, Department of Immunology, Genetics and Pathology, Uppsala University, Uppsala, Sweden** (Prof B Nilsson MD)

Correspondence to: Prof Paolo Macchiarini, Advanced Center for Translational Regenerative Medicine (ACTREM), European Airway Institute, Division of Ear, Nose and Throat (CLINTEC), Karolinska Institutet, Alfred Nobels Allé 8, Huddinge, SE-141 86 Stockholm, Sweden **paolo.macchiarini@ki.se**

See Online for webappendix

See Online for webvideo

at the Karolinska University Hospital (Huddinge, Sweden) with stridor, cough, and respiratory difficulties. The patient, previously treated elsewhere with tumoral debulking surgery and postoperative regional radiation (70 Gy),[6] presented with a recurrence of a primary tracheal mucoepidermoid carcinoma affecting the distal trachea and both main bronchi (figure 1A). The patient underwent an extensive staging,[1] including ^{18}F-fluorodeoxyglucose (^{18}F-FDG) PET scan, multistage biopsies of the respiratory mucosa proximal and distal to the macroscopic tumour burden, and bone marrow biopsy and aspiration. Results showed no local or distant lymphatic or systemic metastasis, and normal stromal cells. The tumour extended from 5 cm above the right tracheobronchial angle into the first 1·3 cm of the right main bronchus, leaving the origins of the upper and intermedius take-offs tumour free, and the first 1·5 cm of the origin of the left main bronchus (webvideo 1). On the basis of surgical standards,[3] this extension was deemed beyond resectability; therefore a transplant procedure, with an artificial biomaterial, was offered to the patient.

We obtained written informed consent from the patient, and the transplant procedure was approved by the local scientific ethics committee.

Pretransplant preparation

We manufactured a tailor-made trachea from the preoperative chest CT and three-dimensional volume rendered images of the patient with a nanocomposite polymer (POSS-PCU; polyhedral oligomericsilsesquioxane [POSS] covalently bonded to poly-[carbonate-urea] urethane [PCU]) processed by an extrusion-phase-inversion method.[7] On the basis of our previous experience with the physical and mechanical properties of human trachea (webappendix p 11)[8] and the patient's preoperative CT scan (figure 1B), we developed a POSS-PCU nanocomposite polymeric airway of appropiate size and morphology, reproducing the exact dimensions of the patient's tracheobronchial structure (webappendix p 12). A Y-shaped three-dimensional glass mandrel was fabricated, and U-shaped rings of POSS-PCU, analogous to the cartilaginous rings of tracheobronchial tissue, were manufactured with casted methodologies and placed around the mandrel. The entire mould was then placed in the POSS-PCU solution to form a coagulated porous scaffold.

A bioreactor to accommodate precisely the maturation requirements of the Y-shaped synthetic windpipe construct used in the transplantation was developed (Hugo Sachs Elektronik-Harvard Apparatus GmbH, March-Hugstetten, Germany; figure 1C, D). The design was based on a sterilisable rotating-construct bioreactor, previously validated but with novel elements to drive a recirculating fluid flow within and around the developing graft,[5] enabling consistent and uniform delivery of cells, nutrients, gases, and hydrodynamic shear forces within the bioreactor. This process is accomplished without external fluid pumps and packaged within the bioreactor assembly so that ease of handling and simplicity of use in good manufacturing practice and clinical environments is not compromised.

Autologous MNCs were obtained 2 days before transplantation from a bone marrow aspirate through density gradient separation. Analyses of white blood cells, mononuclear cells, CD34+ cells, viability, colony-forming unit-fibroblast, flow cytometric characterisation, and sterility were done. To obtain the synthetic bioengineered tracheobronchial construct, cells were resuspended in low-glucose Dulbecco's modified Eagle's medium (Invitrogen, Stockholm, Sweden) and seeded onto the synthetic graft by incubation of the construct in the bioreactor at 37°C for 36 h before transplantation.

Immediately before transplantation, a second bone marrow harvest was done, and MNCs were separated and transferred to the operating theatre. Immediately before implantation, the airway construct was transported to the operating theatre, reseeded with the obtained MNCs, and conditioned with growth and regenerative factors—namely, recombinant human transforming growth factor-β3 (R&D Systems, Minneapolis, MN, USA; 10 μg/cm²), granulocyte-colony stimulating factor filgrastim (G-CSF, Neupogen; Amgen Europe BV, Breda, Netherlands; 10 μg/kg), and epoetin beta (analogous synthetics of Erythropoietin Roche, Grenzach-Wyhlen, Germany; 40 000 UI). We assessed sections of the graft, surplus to clinical need, by scanning electron microscopy, fluorescence, and bright field light microscopy and confocal live cell imaging (webappendix pp 14–15; webvideo 2).

Transplantation

Under general anaesthesia and orotracheal intubation, a redo sternotomy was done and the tumour-burden area dissected and mobilised, according to the principles of tracheal surgery.[1–3] Because of the previous postsurgical and radiation-induced scar tissue formation, the tumour had to be resected along with the right intrapericardial pulmonary artery, and subsequently revascularised with a Dacron 8F graft (Gelsoft, Vascutek, Terumo, Ann Arbor, MI, USA). The graft was interposed between the retroaortic and the extrapleural origin of the pulmonary artery, clamping both vena cavae for 26 min and without use of cardiopulmonary bypass. Tumour resection included the postlateral and mediastinal aspect of the distal truncus of the superior vena cava via lateral clampage and direct suture. The resected trachea included its distal intrathoracic 6 cm, the entire right main bronchus, and first 2 cm of the left main bronchus. All tumour margins were negative on frozen section, and a complete mediastinal lymph-node dissection was done. The airway was then reconstructed by implantation of the reseeded nanocomposite end-to-end, first to the right and left main bronchi and then to the proximal trachea, with standard techniques.[3] Finally, the omentum major was wrapped around the construct and the median

sternotomy and laparotomy closed in a standard manner. From our past experience with carinal surgery when cough reflex, mucous clearance, and patient's full mobilisation are suboptimal in the early postoperative course, a temporary tracheotomy above the implanted graft was made at the end of the procedure.[9]

Regenerative boosting therapy

To enhance the regenerative process, the patient was treated pharmacologically by subcutaneous injections of G-CSF (10 µg/kg) and epoetin-alpha (40 000 UI), with a loading dose given the day before transplantation and every other day for 2 weeks during the postoperative period.

Follow-up assessment

Control endoscopies were done postoperatively daily for the first 7 days, for inspection of the graft and anastomoses. Bronchoscopies were then done once a week during admission to hospital, and once a month thereafter. Postoperative biopsies of the bioartificial graft were assessed by immunohistochemistry, haematoxylin-eosin stain, periodic acid-Schiff stain, and Masson's trichrome stain. Micro-RNA assessment in serum and analyses of soluble factors in plasma (multiplex cytokine assay and ELISA) were done every second day for 2 weeks after transplantation.

Peripheral blood mononuclear cells (PBMCs) were isolated by gradient centrifugation, with Lymphoprep (Nyegaard, Oslo, Norway) and washed twice with phosphate-buffered saline (Gibco, Grand Island, NY, USA). We assessed cell count and viability assays by Türk and trypan blue dye exclusion or by Nucleocounter NC-100 (ChemoMetec A/S, Allerød, Denmark). We analysed gene expression, chromatin immunoprecipitation, and analyses of PBMC subsets and phenotyping 2 days before surgery, and for 2 weeks postoperatively.

Statistical analysis

We undertook data analysis, preparation of graphs, and statistical comparisons with Prism software (Graphpad Prism version 5.0a) and three-dimensional surface modelling with Microsoft Excel 2010.

Role of the funding source

The sponsors of the study had no role in study design, data collection, data analysis, data interpretation, or writing of the report. The corresponding author had full access to all the data in the study and had final responsibility for the decision to submit for publication.

Results

The patient was awake 24 h after transplantation. The immediate postoperative course was characterised by a right upper lobe pneumonia (day 2); *Candida albicans* (>10 000 CFU/mL) and *Stenotrophomonas maltophilia* (>10 000 CFU/mL) were isolated and treated with broad spectrum antibiotics and intensive physiotherapy. Other than this complication, the patient improved gradually and was weaned from the mechanical ventilation on day 5 postoperatively.

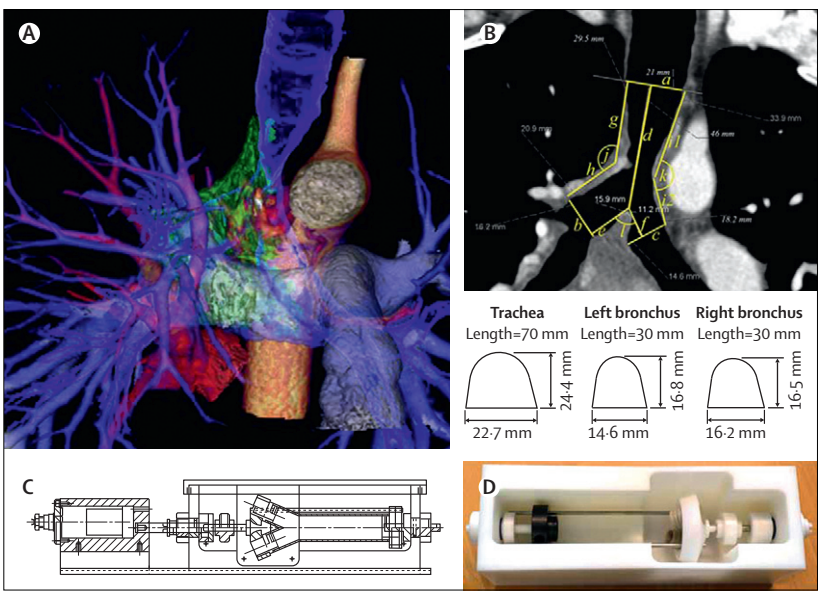

Figure 1: **CT scan and three-dimensional volume rendered (VR) images**
(A) Preoperative VR frontal plane image. Extension of tumour is shown in green. Tracheal and bronchial tree air space is shown in bright blue. The image shows the relation between tumour and right main pulmonary artery. (B, top) Measurement image. An angulated 2 mm thick CT image is used for measurements for individualised scaffold production. The image was optimised for concurrent visualisation of the tumour involvement of trachea inclusive of carina and proximal bronchi aligned parallel to tracheal longitudinal axis. Yellow lines mark proximal trachea (a) and distal right (b) and left (c) bronchi free from tumour involvement, and measurement of the transverse lumen diameters. Sagittal diameter was calculated from angulated transverse image perpendicular to the central lumen line (not shown). (d) Trachea free from tumour (carina); (e) right bronchus free from tumour (carina); (f) left bronchus free from tumour (carina); (g) trachea free from tumour, angle of trachea and right main bronchus; (h) angle of trachea and right main bronchus, right main bronchus free from tumour; (i) 1+2 corresponding left side measurements; (j) angle of trachea and right bronchus; (k) angle of trachea and left bronchus; (l) carinal angle. (B, bottom) Cross section of mandrel for (a) trachea, (b) left bronchus, and (c) right bronchus. (C) Frontal cutaway view of the improved bioreactor. (D) Macroscopic view showing bioreactor without the lid.

1 week after surgery, the bronchoscopy (webvideo 3, figure 2A) showed a normal and patent airway bleeding from its inner layer at the contact with the scope; the obtained biopsy samples showed the presence of necrotic connective tissue associated with fungi contamination and neoformed vessels (figure 2B). The temporary tracheotomy cannula was removed 18 days later. The patient was then transferred to a normal ward and discharged to the referral hospital 1 month after surgery. The biopsy sample 2 months after transplantation showed large granulation areas with initial signs of epithelialisation and more organised vessel formations, and no bacterial or fungi contamination (figure 2B). The patient was discharged from the referring hospital to start rehabilitation and later resumed his university studies. 5 months after transplantation, the patient is asymptomatic, breathes normally, is tumour free, and has an almost normal airway (figure 2C) and improved lung function compared with preoperatively (table, webappendix p 16).

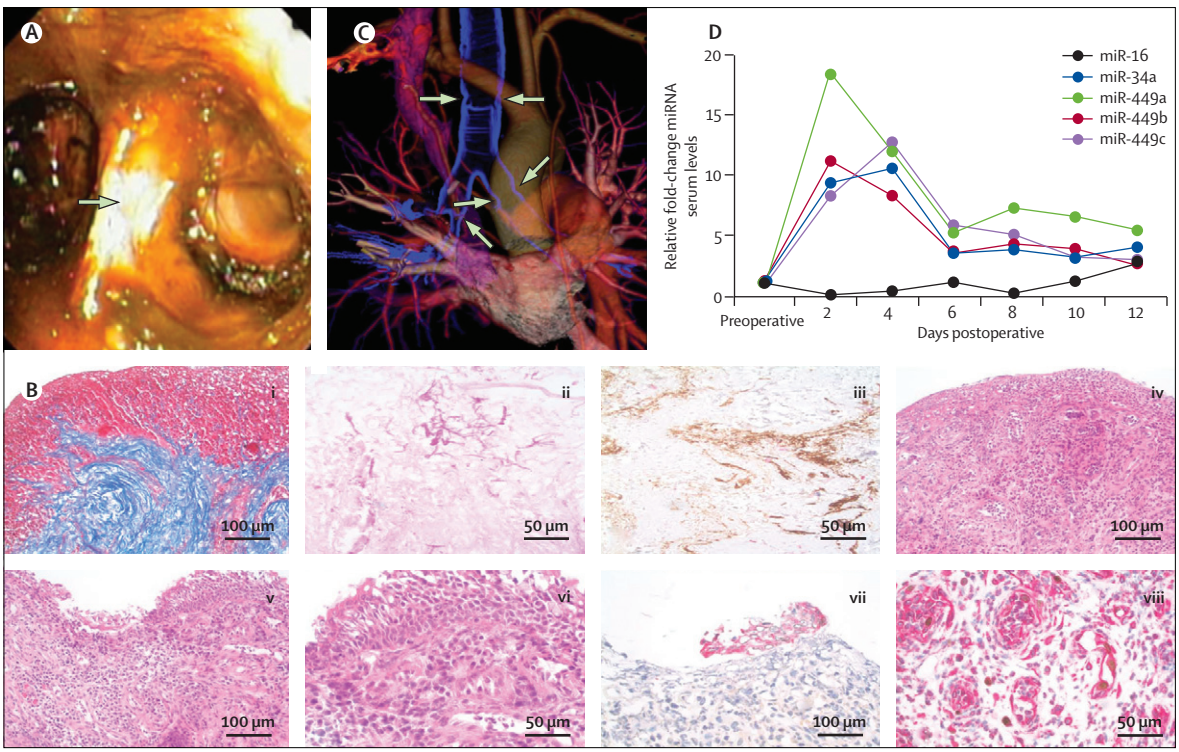

Figure 2: **Postoperative follow-up**
(A) Bronchoscopy image showing the transplanted bioengineered construct integrated with surrounding tissues. (B) Histological evaluation (Masson) of the first postoperatively obtained biopsy sample (at day 7) from the distal part of the graft showed necrotic connective tissue (i) with fungi contamination (periodic acid-Schiff stain; ii) but developed vascular structure (CD146 with Bond Polymer Refine Detection brown colour; NGFR with Bond Polymer Refine Red Detection red colour [without stained structures]; immunolabelling was done on Leica -Bond-Max automated immunostainer; iii). By contrast, the follow-up biopsy at 2 months (haematoxylin-eosin stain) showed ulceration with granulation tissue (iv) and still inflammation, but also respiratory epithelium with mucus secreting cells (haematoxylin-eosin stain; v and vi). Additionally, P63-DAB/CK17 staining showing detached metaplastic squamous epithelium (red; vii) and Mib1-DAB/Vimentin staining showing proliferating (brown) endothelial structures in capillaries. (C) Postoperative volume rendered (VR) image. Air in airways is shown in bright blue. Note that the VR technique displays only the factual air and not the scaffold material. Yellow arrows show borders for scaffold insertion. (D) Serum levels of miR-16, miR-34, miR-449b, and miR-449c were measured by quantitative PCR in serum samples gained at the indicated timepoints before and after surgery.

	May, 2011 (before surgery)	October, 2011 (4 months after surgery)
FVC (L)	3·80	2·63
FEV_1 (L)	1·52	1·95
FEV_1:FVC (%)	40·02%	74·37%

FVC=forced vital capacity. FEV_1=forced expiratory volume in 1 s.

Table: **Lung function tests**

Analyses by micro-RNA expression have shown that serum levels of miR-34 and miR-449 members are potential biomarkers for promotion of terminal differentiation of airway epithelium.[10] Compared with preoperative levels, we noted upregulation 2 days after transplantation, which gradually decreased (figure 2D). By contrast, serum levels of miR-16—a ubiquitous miRNA frequently used for normalisation of serum miRNA levels[11]—remained unchanged.

The autologous bone marrow MNCs were seeded on the synthetic graft and incubated in the bioreactor (webappendix p 14), resulting in a bioengineered tracheobronchial construct suitable for transplantation (webappendix p 17). Scanning electron microscopy of cells incubated in the bioreactor and confocal microscopy of live cells statically exposed to the biomaterial identified cells of different morphologies inside the scaffold, including long processes, filopodia, and lamellipodia (webappendix pp 16–17), whose formation requires anchorage to the scaffold. Although a shortage in material prevented us from undertaking a thorough analysis of cell division, some of the observed cells seemed to be newly divided (webappendix p 17) and cells exposed to the bioreactor aggregated in dense clusters, suggesting clonal expansion. Staining with the CD105 marker showed a subpopulation of cells of mesenchymal lineage (webappendix p 17). Flow cytometric phenotyping of the bioreactor medium showed a selective reduction of MSCs and haemopoietic stem cells (HSCs) after the reseeding process, with a particular decrease in CD90 high and CD59 dim cells (webappendix p 17), suggesting their preferential attachment and engraftment to the scaffold.

Monitoring of patient cell counts and plasma markers showed formation of typical acute phase reactants,

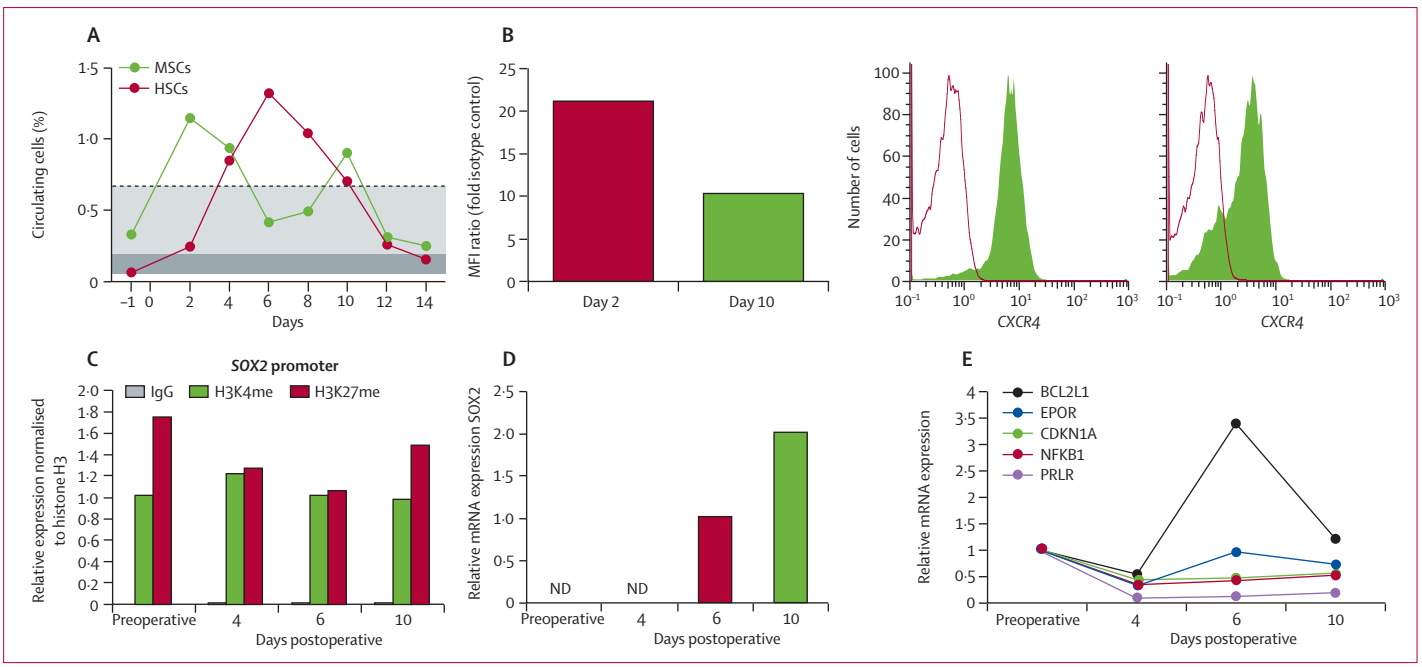

Figure 3: **Analysis of peripheral blood mononuclear cells after surgery (flow cytometry, gene expression, and epigenetic regulation)**
(A) Dynamics of circulating MSCs and haemopoietic stem cells (HSCs) as analysed by high-resolution flow cytometry. MSCs in circulation reached a peak level 2 days after surgery and subsequently decreased, and thereafter reached a secondary peak at day 10. The detection ranges from four healthy donors matched for age and sex (male donors aged from 32–39 years, randomly selected at the Karolinska Institutet, Stockholm, Sweden) are shown in light grey. The percentage of circulating HSCs increased and reached to a plateau at day 6 but then rapidly decreased to normal levels at day 14. Reference ranges assessed from four donors are shown in dark grey. (B) Expression of CXCR4 on circulating MSCs on days 2 and 10 as acquired by flow cytometry. Left panel: comparison of mean fluorescence intensity (MFI) ratios on days 2 and 10. Right and centre panels: red lines indicate isotype controls and green histograms indicate MSCs. (C) Quantitative PCR results after chromatin immunoprecipitation procedure using antibodies against histone H3 (for normalisation), trimethylated lysine 4 (H3K4me3), and trimethylated lysine 27 (H3K27me3) on histone 3 at the promoter regions of the gene *SOX2*. (D) Expression of the SOX2 gene relative to GAPDH, analysed by quantitative RT-PCR. (E) Fold change of genes with antiapoptotic function, relative to the preoperative condition, analysed by quantitative RT-PCR array. ND=not detectable.

wounding, tissue remodelling, and regenerative factors after surgery (webappendix pp 18–19). Webappendix p 19 shows results of a heat map analysis with the exact kinetics and numerical values for individual factors. Findings from a flow cytometric analysis of the peripheral blood showed an increase in HSCs at day 6, with a particular increase of the CD90+ subpopulation (webappendix pp 20–21). We noted an increased amount of circulating MSCs at day 2, to 15-fold higher levels than the age and sex matched healthy donor range (figure 3A), possibly as a result of the boosting therapy before surgery; this increase was followed by a three-fold decrease at day 4 and 6, to show a secondary two-fold increase at day 10. In line with these findings, the relative gene expression of homing-associated factor SDF-1 receptor CXCR4 was two-fold higher in MSCs at day 2 than at day 10 (figure 3B).

We then undertook a molecular analysis of the stem-cell phenotype. Chromatin immunoprecipitation showed that the *SOX2* gene, encoding a progenitor-associated transcription factor, showed stable concentrations of the H3K4me3 activity mark throughout the postoperative analysis. However, the H3K27me3 repressive mark was decreased in samples retrieved 4 and 6 days after surgery, showing an increased activity and decreased repression at these timepoints (figure 3C). Accordingly, this increased total activity preceded an induction of SOX2 gene expression at day 6 and a further increase at day 10 (figure 3D). Another progenitor-associated gene, GNL3, also displayed an increasing ratio of active and repressive marks H3K4me3 and H3K27me3 at day 6, correlating with increased gene expression (data not shown). These results on chromatin state and gene expression lend support to the flow cytometric analysis indicating a second wave of circulating MSCs (figure 3A, webappendix p 20).

We investigated the expression in PBMCs of genes involved in the JAK/STAT pathway—a major signalling transduction pathway activated by epoetin beta. Most genes showed a consistent trend of downregulation at day 4 postoperatively, compared with the preoperative condition, with subsequent progressive recovery of the expression levels at days 6 and 10 (webappendix p 22). Analysis of antiapoptotic genes showed a peak in the expression of BCL2L1 and EPOR at day 6, suggesting increased antiapoptotic activity in PBMCs at that time (figure 3E).

Discussion

Findings from this proof-of-concept case study show the feasibility of tracheal transplantation with an artificial nanocomposite reseeded with autologous stromal cells.

Panel: **Research in context**

Systematic review

We searched Medline and PubMed without date or language restrictions for articles with the following terms: "trachea", "tracheal replacement", "tracheal cancer", "tracheal surgery", "transplantation", "stem cells", "cell mobilization", "tissue engineering", "scaffold", and "synthetic material". We identified several relevant articles showing challenges and outcome of tracheal reconstruction and replacement, published between 1997 and 2011.[3,4,9,10,20,21,23–25] However, we could not locate any report showing the successful transplantation of a cell-seeded synthetic scaffold-based tracheal transplantation in human beings. Moreover, we identified no publication showing detailed insights into active stem-cell mobilisation in tracheal transplanted patients.

Interpretation

Our study is the first to describe a successful transplantation of a synthetic-based stem-cell seeded scaffold in a patient. Our data were collected from preoperative and postoperative in-vivo measurements and in-vitro studies. We applied complementary methods to confirm findings. Even though we now describe only one case of tissue-engineered tracheal transplantation, the magnitude of data and the validation of a specific mechanism suggest solid evidence. Our specific findings are verified and discussed extensively in relation to earlier findings from independent investigators. Moreover, our data provide novel insights into cellular pathways.

We have also shown the possibility of stem-cell mobilisation and the dynamic patterns and profile of mononuclear cells in peripheral blood circulation. Despite much progress in the clinical translation of tissue engineered organs and complex tissues,[12,13] no safe and suitable solution has been identified to successfully replace the trachea.[14,15] With a human decellularised tracheal matrix, repopulated with in-vitro expanded and differentiated autologous chondrocytes of MSC origin and autologous epithelial cells via a novel bioreactor system, the first-in-man completely tissue-engineered trachea replacement was successfully done.[5] This strategy, improved by intraoperative graft seeding with autologous cells (bone marrow MSCs and respiratory cells) and conditioning with differentiation and tissue-protective factors,[16] was subsequently successfully used in patients with both benign and malign airway diseases. However, this approach has limitations—eg, a long period for the decellularisation process (15–20 days), the need for different patient-specific sizes, the risks for altering long-term natural matrix mechanical properties, bacterial contamination during the in-vitro natural graft manipulation, and, most importantly, the absolute requirement of obtaining a donor organ.

The primary tumour of our patient involved the last 5 cm of the distal trachea along with the tracheobronchial bifurcation, which represents an absolute contraindication to any surgical resection. Because the patient had a tumour recurrence with severe stridor, despite 70 Gy of radiation therapy, and the waiting time for a donation would have been unpredictable, we decided to attempt a curative surgery by replacement of the resected airway with an artificial POSS-PCU-based nanocomposite combined with a novel pharmacological boosting strategy. This decision was based on the fact that the POSS-PCU is biocompatible, non-toxic, non-biodegradable, inert, and has negligible immunoreactivity.[17] Additionally, it displays mechanical properties, in-vivo chemical stability, and nanostructural features,[18,19] which approach the ideal for a bioengineered tracheal implant. And, it is patient specific, since it could be designed to replace not only the trachea but also the bronchi, or a combination of both. Lastly, it can be produced in a rapid and clinically appropriate timeframe.

Previous attempts to replace the airways of patients with tracheal cancer with synthetic materials have been unsuccesful because of graft's limited cell seeding, infection, migration, stenosis, necrosis, and ultimately death of the patients.[4] These drawbacks are clearly related to the fact that the trachea is not located in a mesenchymal environment, but is in direct contact with the breathing air, making infection and contamination more likely to occur. Thus we used a bioreactor environment to reseed the bioartifical scaffold with autologous mononuclear cells. Results showed that 36 h of dynamic incubation of the mononuclear cells in the bioreactor was sufficient for them to adhere to the biomaterial. 2 days after seeding, the cells exposed to the bioreactor formed dense clusters, whereas those statically incubated were more evenly distributed (webappendix p 17), indicating that the bioreactor might help nested cells to proliferate. Antibody labelling and morphological analysis showed the presence of proliferating CD105+ cells with mesenchymal but not haemopoietic phenotype within the graft. Although an extracellular matrix (ECM)-like structure was observed on the scaffold (webappendix p 17) after the reseeding and bioreactor process, whether this structure is related to the autologous serum or the production of ECM by engrafted cells is unclear.

The most frequently reported airway complications after lung transplantation are necrosis, dehiscence, and stenosis, probably related to ischaemia of the transplanted bronchus during the immediate period after transplantation.[20–22] In this report, an avascularised, Y-shaped nanocomposite was implanted and the initial fungal infection had resolved within 4 months from transplantation; later the endoluminal surface was partly lined with respiratory mucosa, at which we noted nearly healthy epithelium and proliferating endothelium. This finding provides evidence that a bioengineered synthetic tracheobronchial nanocomposite can be recellularised in vivo with site-specific cells to become a living and functional scaffold completely integrated into the adjacent tissues. The measured levels of miR-34/449

micro-RNAs, which have been proposed as potential biomarkers of terminal differentiation of airway epithelium,[10] suggest the presence of postoperative airway epithelial differentiation in the patient.[11]

One of the key issues in a synthetic transplantation setting is the recruitment of repair cells that promote the integration and remodelling of the newly transplanted material. The cellular components contributing to regeneration can be recruited either from local tissue or from circulating progenitor cells. We observed HSC mobilisation together with increased amounts of circulating MSCs, which contrasts with previous findings[23] of no mobilisation of MSCs, when G-CSF was used as mobilising agent alone. Indeed, surgery-induced inflammation and chemokine and anaphylatoxin release at the implantation site could be the reason for the observed MSC mobilisation in our patient. We detected release of a large array of soluble mediators associated with wound healing, which could promote MSC mobilisation, as previously reported by other investigators.[24,25] Additionally, G-CSF induced neutrophil expansion, and release of proteases, which we also detected, could have promoted progenitor mobilisation.[26] Progenitor mobilisation presumably occurs by weakening their anchoring within the niche, either by degradation of the anchoring ECM components or their retention factor SDF-1a itself.[26] Bone marrow progenitor cell activation, recruitment, tissue repair, and local immune suppression at the surgery site could be enhanced by blood activation products, such as C3a and thrombin,[26–28] which were formed upon scaffold implantation. We detected a strong systemic release of growth factors and matrix metalloproteinases, which are probably produced by recruited progenitor and other immune cells. Furthermore, we recorded a substantial and very early increase of the epoetin-receptor expression with simultaneous upregulation of antiapoptotic genes, such as *BCL2L1*. During inflammation, trauma cytokines are released which upregulate epoetin receptors but inhibit tissue protection by downregulation of local epoetin production and antiapoptotic downstream pathways, favouring cell apoptosis. To avoid this early postoperative absence of local epoetin production, we administered regenerative (500 UI/Kg) epoetin doses, aiming to favour and trigger early local tissue protection and regeneration.

Taken together, these results provide evidence that a successful organ regeneration strategy has been accomplished (panel). The successful overall clinical outcome of this first-in-man bioengineered artificial tracheobronchial transplantation provides ongoing proof of the viability of this approach, in which a cell-seeded synthetic graft is fabricated to patient-specific anatomical requirements and incubated to maturity within the environment of a bioreactor. Additionally, in-depth cellular biochemistry analyses have provided new insight into the mechanisms by which the so-called pharmacological boosting factors contribute to cell mobilisation, differentiation, and ultrastructural organisation of the fully engrafted tracheobronchial construct.

Contributors

PJ was responsible for the bioreactor-based cell seeding; assisted the surgery and with collection of secondary data; and wrote corresponding methods, results, and interpretation sections. EA and TS undertook all flow cytometry characterisation of the cells, interpreted the results, and wrote corresponding methods. SB provided preclinical data for human tracheal biomechanics, and helped to write the report. KLB, BN, and GM designed, undertook, and assessed the multiplex analyses and wrote corresponding methods. KLB undertook the bone-marrow isolation. PB organised and supervised standards at the good manufacturing practice facility. BB did histological evaluation. CC and AS designed and developed the three-dimensional nanocomposite trachea, and wrote corresponding methods. OE and TG are responsible for the clinical follow-up of the patient and provided biopsy material and blood samples; TG also participated in the surgery and wrote corresponding methods. K-HG and JL assisted the surgery. SLG and SS did all cell imaging and wrote corresponding methods. OH and TL undertook and assessed all epigenetic analyses and wrote corresponding methods. JEJ and GH assisted in the preoperative and postoperative care. BL did all radiological imaging, interpretation, and three-dimensional reconstruction, and wrote corresponding methods. TL and CR undertook and assessed the miRNA studies, and wrote corresponding methods. VL and AIT undertook and analysed gene expression experiments, and wrote corresponding methods. EW isolated the mononuclear cells. PM was the primary investigator and leading author of the report, indicated how to built the three-dimensional nanocomposite, was leading surgeon and was responsible for the preoperative and postoperative course, and oversaw the review process. All authors provided primary data for modelling scenarios, and assisted with interpretation of results and report revision.

Conflicts of interest

We declare that we have no conflicts of interest.

Acknowledgments

The European Commission (FP7 EU Project: 280584-2BIOtracheaCP-FPFP7-NMP-2011-SMALL-5), the Knut and Alice Wallenberg Foundation, Swedish Research Council, and the StratRegen funded preclinical and postoperative in-vitro studies, gene expression, cell characterisation, and imaging. The Vinnova Foundation, Radiumhemmet, and Clinigene EU Network of Excellence funded multiplex and flow cytometric analyses. The Swedish Cancer Society supported the epigenetic studies. The Centre for Biosciences, the Knut and Alice Wallenberg Foundation, and the Swedish Research Council supported the Live Cell imaging Unit at the Department of Biosciences and Nutrition, Karolinska Institutet, used for live cell imaging. ERC-2007-Stg/208237-Luedde-Med3-Aachen funded the miRNA studies. The UCL Business supported the development of the three-dimensional nanocomposite scaffold. We thank all the health professionals of the Karolinska University Hospital in Huddinge, Stockholm, Sweden, without whom the transplantation could not have been done; Harvard Apparatus (Hollison, MA, USA) and Hugo Sachs Elektronik-Harvard Apparatus GmbH (March-Hugstetten, Germany) for supporting us with the bioreactor and the supervision of its use; Peter Güntner, for image analysis and measurements for scaffold production, and Anders Svensson, for three-dimensional volume image rendering, both from the Department of Radiology, Karolinska University Hospital Huddinge, Stockholm, Sweden; all the staff of the Landspitali University Hospital in Reykjavik, for the excellent support with the preoperative and postoperative care of the patient; Alessandra Bianco and Costantino Del Gaudio from Department of Science and Chemical Technologies, Intrauniversitary Consortium for Material Science Technology (INSTM), Research Unit Tor Vergata, Rome, Italy, for bi-dimensional and three-dimensional mathematical model for tracheal lateral area assessment; Iyadh Douagi from the Center of Hematology and Regenerative Medicine, Department of Medicine, Karolinska Insitutet for his assistance with flow cytometry; and Ulrika Felldin from ACTREM, Karolinska Institutet for her assistance with cell isolation.

References

1 Macchiarini P. Primary tracheal tumours. *Lancet Oncol* 2006; **7:** 83–91.

2 Gaissert HA, Burns J. The compromised airway: tumors, strictures, and tracheomalacia. *Surg Clin North Am* 2010; **90:** 1065–89.

3 Grillo HC. Primary tracheal tumours. In: HC Grillo, ed. Surgery of the trachea and bronchi. Hamilton: BC Decker, 2004: 791–802.

4 Macchiarini P, Jungebluth P, Go T, et al. Clinical transplantation of a tissue-engineered airway. *Lancet* 2008; **372:** 2023–30.

5 Go T, Jungebluth P, Baiguera S, et al. Both epithelial cells and mesenchymal stem cell derived chondrocytes contribute to the survival of tissue-engineered airway transplants in pigs. *J Thorac Cardiovasc Surg* 2010; **139:** 437–43.

6 Sigurdsson MI, Sigurdsson H, Hreinsson K, Simonardottir L, Gudbjartsson T. Bronchiovenous fistula causing bleeding and air embolism: an unusual complication of bronchoscopic tumor resection. *Am J Respir Crit Care Med* 2011; **183:** 681–82.

7 Ahmed M, Ghanbari H, Cousins BG, Hamilton G, Seifalian AM. Small calibre polyhedral oligomeric silsesquioxane nanocomposite cardiovascular grafts: influence of porosity on the structure, haemocompatibility and mechanical properties. *Acta Biomater* 2011; **7:** 3857–67.

8 Baiguera S, Jungebluth P, Burns A, et al. Tissue engineered human tracheas for in vivo implantation. *Biomaterials* 2010; **31:** 8931–38.

9 Macchiarini P, Altmayer M, Go T, et al. Technical innovations of carinal resection for nonsmall-cell lung cancer. *Ann Thorac Surg* 2006; **82:** 1989–97.

10 Lizé M, Herr C, Klimke A, Bals R, Dobbelstein M. MicroRNA-449a levels increase by several orders of magnitude during mucociliary differentiation of airway epithelia. *Cell Cycle* 2010; **9:** 4579–83.

11 Bihrer V, Friedrich-Rust M, Kronenberger B, et al. Serum miR-122 as a biomarker of necroinflammation in patients with chronic hepatitis C virus infection. *Am J Gastroenterol* 2011; **106:** 1663–69.

12 Atala A, Bauer SB, Soker S, Yoo JJ, Retik AB. Tissue-engineered autologous bladders for patients needing cystoplasty. *Lancet* 2006; **367:** 1241–46.

13 Pham C, Greenwood J, Cleland H, Woodruff P, Maddern G. Bioengineered skin substitutes for the management of burns: a systematic review. *Burns* 2007; **33:** 946–57.

14 Behrend M, Kluge E, Von Wasielewski R, Klempnauer J. The mechanical influence of tissue engineering techniques on tracheal strength: an experimental study on sheep trachea. *J Invest Surg* 2002; **15:** 227–36.

15 Gilbert TW, Gilbert S, Madden M, Reynolds SD, Badylak SF. Morphologic assessment of extracellular matrix scaffolds for patch tracheoplasty in a canine model. *Ann Thorac Surg* 2008; **86:** 967–74.

16 Bader A, Macchiarini P. Moving towards in situ tracheal regeneration: the bionic tissue engineered transplantation approach. *J Cell Mol Med* 2010; **14:** 1877–89.

17 de Mel A, Punshon G, Ramesh B, et al. In situ endothelialization potential of a biofunctionalised nanocomposite biomaterial-based small diameter bypass graft. *Biomed Mater Eng* 2009; **19:** 317–31.

18 Seifalian AM, Salacinski HJ, Tiwari A, Edwards A, Bowald S, Hamilton G. In vivo biostability of a poly(carbonate-urea) urethane graft. *Biomaterials* 2003; **24:** 2549–57.

19 Kannan RY, Salacinski HJ, Butler PE, Seifalian AM. Polyhedral oligomeric silsesquioxane nanocomposites: the next generation material for biomedical applications. *Acc Chem Res* 2005; **38:** 879–84.

20 Kshettry VR, Kroshus TJ, Hertz MI, Hunter DW, Shumway SJ, Bolman RM III. Early and late airway complications after lung transplantation: incidence and management. *Ann Thorac Surg* 1997; **63:** 1576–83.

21 Santacruz JF, Mehta AC. Airway complications and management after lung transplantation: ischemia, dehiscence, and stenosis. *Proc Am Thorac Soc* 2009; **6:** 79–93.

22 Puchalski J, Lee HJ, Sterman DH. Airway complications following lung transplantation. *Clin Chest Med* 2011; **32:** 357–66.

23 Pitchford SC, Furze RC, Jones CP, Wengner AM, Rankin SM. Differential mobilization of subsets of progenitor cells from the bone marrow. *Cell Stem Cell* 2009; **4:** 62–72.

24 Mansilla E, Marin GH, Drago H, et al. Bloodstream cells phenotypically identical to human mesenchymal bone marrow stem cells circulate in large amounts under the influence of acute large skin damage: new evidence for their use in regenerative medicine. *Transplant Proc* 2006; **38:** 967–69.

25 Hannoush EJ, Sifri ZC, Elhassan IO, et al. Impact of enhanced mobilization of bone marrow derived cells to site of injury. *J Trauma* 2011; **71:** 283–91.

26 Marquez-Curtis LA, Turner AR, Sridharan S, Ratajczak MZ, Janowska-Wieczorek A. The ins and outs of hematopoietic stem cells: studies to improve transplantation outcomes. *Stem Cell Rev* 2011; **7:** 590–607.

27 Schraufstatter IU, Discipio RG, Zhao M, Khaldoyanidi SK. C3a and C5a are chemotactic factors for human mesenchymal stem cells, which cause prolonged ERK1/2 phosphorylation. *J Immunol* 2009; **182:** 3827–36.

28 Moll G, Jitschin R, von Bahr L, et al. Mesenchymal stromal cells engage complement and complement receptor bearing innate effector cells to modulate immune responses. *PLoS One* 2011; **6:** e21703.